

Low-Temperature Syntheses and Characterization of Novel Layered Tellurites, $A_2Mo_3TeO_{12}$ ($A = NH_4, Cs$), and “Zero-Dimensional” Tellurites, $A_4Mo_6Te_2O_{24} \cdot 6H_2O$ ($A = Rb, K$)

Vidyavathy Balraj and K. Vidyasagar*

Department of Chemistry, Indian Institute of Technology Madras, Chennai 600 036, India

Received January 28, 1998

Hydrothermal synthetic investigations to prepare new $A_2Mo_3TeO_{12}$ ($A = NH_4, Cs, Rb, K$) compounds are described. Novel noncentrosymmetric layered tellurites, $(NH_4)_2Mo_3TeO_{12}$ (**1**) and $Cs_2Mo_3TeO_{12}$ (**2**), have been synthesized by hydrothermal methods. Their structures contain two-dimensional hexagonal tungsten oxide related $(Mo_3TeO_{12})^{2-}$ anionic layers interleaved with NH_4^+/Cs^+ ions. New “zero-dimensional” tellurites, $Rb_4Mo_6Te_2O_{24} \cdot 6H_2O$ (**3**) and $K_4Mo_6Te_2O_{24} \cdot 6H_2O$ (**4**), containing discrete centrosymmetric $(Mo_6Te_2O_{24})^{4-}$ anionic aggregates and alkali metal ions have been synthesized by simple refluxing of stoichiometric reactants in water. In this hexamolybdodite tellurite anion, the Mo_6O_{24} flat hexagonal ring, formed from edge sharing of six MoO_6 octahedra, is capped by tellurium on both sides. The two types of anions have the same empirical formula. $Cs_2Mo_3TeO_{12}$ (**2**) could be prepared by a solid state reaction as well. All four new tellurites have been structurally characterized by single-crystal X-ray diffraction studies. Pertinent crystal, data are as follows: for **1**, hexagonal space group $P6_3$, $a = 7.332(2)$ Å, $c = 12.028(4)$ Å, $Z = 2$; for **2**, hexagonal space group $P6_3$, $a = 7.3956(10)$ Å, $c = 12.186(2)$ Å, $Z = 2$; for **3**, monoclinic space group $P2_1/c$, $a = 10.0564(14)$ Å, $b = 9.877(8)$ Å, $c = 15.724(3)$ Å, $\beta = 109.988(11)^\circ$, $Z = 2$; for **4**, monoclinic space group $P2_1/c$, $a = 9.878(3)$ Å, $b = 9.724(4)$ Å, $c = 15.301(3)$ Å, $\beta = 108.57(2)^\circ$, $Z = 2$. Low-temperature syntheses, structure, and powder X-ray diffraction, spectroscopic, and thermal studies of compounds **1–4** are described.

Introduction

Crystalline inorganic solids with one- to three-dimensional framework structures, in their metastable form, are often prepared by low-temperature synthetic routes.¹ The hydrothermal method is one such low-temperature technique that continues to be widely employed in the synthesis of microporous materials such as zeolites. Recently, this method has found broader application in the synthesis of a variety of inorganic oxide materials such as metal phosphates,² phosphonates,^{3,4} and selenites.^{5–9} The metastable materials thus prepared have been shown to possess novel low-dimensional or three-dimensional framework structures. In this method, the variable synthetic

parameters such as type, ratio, and concentration of reactants, temperature and duration of heating, and pH are so many that it could be possible to synthesize a number of phases in a given system. However, the desired phase in pure form, in some cases, could be synthesized only in a very narrow window of synthetic parameters. It thus requires a number of trials to be made for the optimization of the synthetic procedure.

Jacobson and other workers recently reported the hydrothermal synthesis and characterization of two-dimensional novel phosphonates⁴ and selenites^{5–8} of molybdenum, tungsten, and vanadium. These compounds have two interesting features. One is their noncentrosymmetric layered structure based on the hexagonal tungsten oxide motif of corner-shared transition metal–oxygen octahedra, and the other is their nonzero powder-second-harmonic-generation response. The corresponding tellurites have not been reported so far. Unlike Se^{4+} , which exists as mostly pyramidal SeO_3 in oxides, Te^{4+} is known to exhibit, in oxides, a variety of coordinations such as pyramidal TeO_3 , TeO_4 with SF_4 geometry, and TeO_5 square pyramids. The tellurites are, therefore, more interesting from the structural point of view. As a part of our ongoing research on low-temperature synthetic routes for oxide materials, we have attempted the synthesis of tellurite analogues of those hexagonal tungsten oxide (HTO) related selenites by various methods including the hydrothermal technique. In this process, we have isolated a variety of new phases possessing “zero-” to three-dimensional framework structures in the $A/M/Te/O$ ($A =$ alkali metal, Tl, NH_4 ; $M =$ transition metal) systems. In this paper, we report the synthesis and characterization of four novel molybdenum-(VI) tellurite compounds, namely the two-dimensional tellurites $(NH_4)_2Mo_3TeO_{12}$ (**1**) and $Cs_2Mo_3TeO_{12}$ (**2**) and the “zero-

- (1) (a) Rao, C. N. R.; Gopalakrishnan, J. *New directions in solid-state chemistry*; Cambridge University Press: Cambridge, U.K., 1986. (b) Gopalakrishnan, J. *Chem. Mater.* **1995**, *7*, 1265. (c) Kanatzidis, M. G.; Sutorik, A. C. *Prog. Inorg. Chem.* **1995**, *43*, 151.
- (2) Soghomonian, V.; Chen, Q.; Zhang, Y.; Haushalter, R. C.; O'Connor, C. J.; Tao, C.; Zubieta, J. *Inorg. Chem.* **1995**, *34*, 3509.
- (3) (a) Bonavia, G.; Haushalter, R. C.; O'Connor, C. J.; Zubieta, J. *Inorg. Chem.* **1996**, *35*, 5603. (b) Drumel, S.; Janvier, P.; Deniaud, D.; Bujoli, B. *J. Chem. Soc., Chem. Commun.* **1995**, 1051.
- (4) (a) Harrison, W. T. A.; Dussack, L. L.; Jacobson, A. J. *Inorg. Chem.* **1995**, *34*, 4774. (b) Harrison, W. T. A.; Dussack, L. L.; Jacobson, A. J. *Inorg. Chem.* **1996**, *35*, 1461.
- (5) Vaughney, J. T.; Harrison, W. T. A.; Dussack, L. L.; Jacobson, A. J. *Inorg. Chem.* **1994**, *33*, 4370.
- (6) (a) Harrison, W. T. A.; Dussack, L. L.; Jacobson, A. J. *Inorg. Chem.* **1994**, *33*, 6043. (b) Dussack, L. L.; Harrison, W. T. A.; Jacobson, A. J. *Mater. Res. Bull.* **1996**, *31*, 249.
- (7) Harrison, W. T. A.; Dussack, L. L.; Vogt, T.; Jacobson, A. J. *J. Solid State Chem.* **1995**, *120*, 112.
- (8) Kwon, Y.-U.; Lee, K.-S.; Kim, Y. H. *Inorg. Chem.* **1996**, *35*, 1161.
- (9) (a) Harrison, W. T. A.; Vaughney, J. T.; Jacobson, A. J.; Goshorn, D. P.; Johnson, J. W. *J. Solid State Chem.* **1995**, *116*, 77. (b) Lee, K.-S.; Kwon, Y.-U.; Namgung, H.; Kim, S.-H. *Inorg. Chem.* **1995**, *34*, 4178.

Table 1. Reaction Conditions and Products of Hydrothermal Attempts for $A_2Mo_3TeO_{12}$ ($A = NH_4, Cs$) Compounds

A	reacn code	A:Mo:Te	temp (°C)	time (days)	products
NH ₄	A1	1.71:2:1	225	7	(NH ₄) ₂ Mo ₃ TeO ₁₂ (1) (few crystals), (NH ₄) ₄ Mo ₆ TeO ₂₂ ·2H ₂ O (A), hexagonal phase (B)
	A2	2.57:3:1	225	7	1 (41%), A, B
	A3	5.14:6:1	225	7	1 (87.5%), A (very small amount)
	A4	5.14:6:1	235	14	1 (91%), A (very small amount)
	A5	5.14:6:1	225	4	A (1.29 g), B (0.05 g)
Cs	C1	2:3:1	225	7	mixture of white and yellow solids
	C2	4:4:1	225	7	Cs ₂ Mo ₃ TeO ₁₂ (2) (87%), small amount of white powder (C)
	C3	4:4:1	235	14	2 (87%), C (very small amount)
	C4	6:5:1	225	6	2 (72.1%), C (very small amount)

Table 2. X-ray Powder Diffraction Patterns of (NH₄)₂Mo₃TeO₁₂ and Cs₂Mo₃TeO₁₂

(NH ₄) ₂ Mo ₃ TeO ₁₂						Cs ₂ Mo ₃ TeO ₁₂		
<i>h</i>	<i>k</i>	<i>l</i>	<i>d</i> _{cal} ^a (Å)	<i>d</i> _{obs} (Å)	<i>I</i> / <i>I</i> ₀	<i>d</i> _{cal} ^b (Å)	<i>d</i> _{obs} (Å)	<i>I</i> / <i>I</i> ₀
1	0	0	6.3489	6.3454	82	6.4032	6.3933	8
0	0	2	6.0100	6.0053	37	6.1017	6.1027	17
1	0	1	5.6139	5.6100	39			
1	0	2	4.3646	4.3640	18			
1	1	0				3.6969	3.6996	27
1	1	1	3.5061	3.5054	16	3.5381	3.5382	8
1	0	3	3.3883	3.3916	16	3.4335	3.4323	59
2	0	0				3.2016	3.2014	13
1	1	2	3.1294	3.1300	100	3.1618	3.1631	100
2	0	1	3.0692	3.0713	84	3.0968	3.0983	68
0	0	4	3.0050	3.0059	69	3.0509	3.0498	18
2	0	2	2.8069	2.8077	84	2.8350	2.8383	13
1	0	4	2.7161	2.7165	57	2.7542	2.7528	23
1	1	3				2.7359	2.7364	9
2	0	3	2.4881	2.4900	12			
2	1	0	2.3996	2.4004	13	2.4202	2.4234	5
2	1	1	2.3532	2.3527	5	2.3739	2.3749	5
1	0	5	2.2482	2.2482	5	2.2806	2.2796	9
2	1	2	2.2286	2.2291	8	2.2497	2.2507	6
3	0	0				2.1344	2.1352	4
3	0	1	2.0842	2.0855	6			
2	1	3	2.0587	2.0601	5	2.0799	2.0813	19
1	1	5	2.0102	2.0119	5			
0	0	6	2.0033	2.0047	10	2.0339	2.0317	8
3	0	2	1.9961	1.9969	23	2.0147	2.0165	27
2	0	5	1.9165	1.9181	27	1.9410	1.9413	29
2	1	4	1.8751	1.8770	16	1.8960	1.8974	12
2	2	0	1.8328	1.8344	19	1.8484	1.8505	49
3	1	0	1.7609	1.7603	24			
3	1	1	1.7423	1.7443	9			
2	0	6	1.6942	1.6954	21	1.7168	1.7173	23
3	1	2	1.6898	1.6910	21	1.7052	1.7062	7
3	1	3	1.6120	1.6132	13	1.6276	1.6292	20
4	0	1				1.5872	1.5888	9
2	2	4	1.5647	1.5666	18	1.5809	1.5819	6
2	1	6	1.5379	1.5395	8	1.5571	1.5577	7
4	0	2				1.5484	1.5489	6
3	1	4	1.5192	1.5208	7	1.5348	1.5361	14
2	0	7	1.5103	1.5118	8	1.5311	1.5314	10
0	0	8	1.5025	1.5036	7			

^a $a = 7.3310(32)$ and $c = 12.0199(67)$ Å of hexagonal cell. ^b $a = 7.3938(31)$ and $c = 12.2035(70)$ Å of hexagonal cell.

dimensional” tellurites Rb₄Mo₆Te₂O₂₄·6H₂O (**3**) and K₄Mo₆Te₂O₂₄·6H₂O (**4**). The term “zero-dimensional” is being used, in the present context, to denote the discrete nature of (Mo₆Te₂O₂₄)⁴⁻ anionic aggregates which do not have extended framework structures. Such terminology has been used by Muller and co-workers¹⁰ to describe the discrete host structures in polyoxometalates and others.

Table 3. X-ray Powder Diffraction Pattern of Rb₄Mo₆Te₂O₂₄·6H₂O

<i>h</i>	<i>k</i>	<i>l</i>	<i>d</i> _{cal} (Å)	<i>d</i> _{obs} (Å)	<i>I</i> / <i>I</i> ₀	<i>h</i>	<i>k</i>	<i>l</i>	<i>d</i> _{cal} (Å)	<i>d</i> _{obs} (Å)	<i>I</i> / <i>I</i> ₀
1	0	0	9.451	9.448	38	3	2	-2	2.766	2.763	8
0	1	1	8.211	8.216	26	2	0	-6	2.574	2.569	10
0	0	2	7.389	7.381	12	2	2	-5	2.571		
1	0	-2	7.120	7.115	26	4	1	0	2.298	2.295	9
1	1	-1	6.879	6.873	16	3	2	2	2.297		
0	1	2	5.916	5.914	12	3	3	-3	2.293		
1	1	1	5.687	5.684	16	2	3	3	2.195	2.192	14
1	0	2	5.044	5.042	12	2	4	0	2.188		
0	2	0	4.938	4.933	11	1	2	6	2.014	2.011	12
2	0	0	4.725	4.723	10	2	4	2	2.013		
2	1	-1	4.480	4.477	13	2	2	5	2.003	2.001	11
1	2	0	4.377	4.370	13	2	3	4	2.002		
2	1	0	4.263	4.256	11	1	0	-8	1.942	1.941	16
1	2	0	4.377	4.370	13	5	1	-4	1.941		
2	1	0	4.263	4.256	11	3	3	-6	1.925	1.921	15
2	0	-4	3.560	3.559	27	5	1	-1	1.924		
2	2	-1	3.523	3.519	27	4	3	0	1.920		
0	2	3	3.487	3.484	25	1	1	-8	1.906	1.903	16
3	1	-3	3.040	3.039	20	1	5	-2	1.903		
0	3	2	3.007	2.999	100	1	5	1	1.900		
3	1	0	3.001			2	5	-2	1.826	1.823	6
1	1	-5	2.995			2	5	0	1.823		
1	3	-2	2.988	2.984	100	4	4	-2	1.761		
0	2	4	2.958	2.953	44	0	4	6	1.744	1.743	13
1	1	4	2.958			4	3	2	1.744		
2	2	-4	2.888	2.887	12	4	0	4	1.739	1.737	14
2	2	2	2.843	2.840	26	6	2	-6	1.520	1.520	8
						3	5	-6	1.518		
						5	3	2	1.509	1.508	9

Experimental Section

Synthesis. The following chemicals of high purity were used for the synthesis: Cs₂CO₃, Rb₂CO₃, K₂CO₃, TeO₂, MoO₃, and (NH₄)₆Mo₇O₂₄·4H₂O. Teflon-lined 23-mL-capacity acid digestion bombs from Parr were used for hydrothermal synthesis. Some of the hydrothermal synthetic attempts made for (NH₄)₂Mo₃TeO₁₂ (**1**) and Cs₂Mo₃TeO₁₂ (**2**) are listed in Table 1. The final pH in all the standardized procedures was neutral. The syntheses were carried out by hydrothermal, refluxing, and ceramic methods.

(10) Muller, A.; Reuter, H.; Dillinger, S. *Angew. Chem., Int. Ed. Engl.* **1995**, *34*, 2328.

Table 4. X-ray Powder Diffraction Pattern of $K_4Mo_6Te_2O_{24} \cdot 6H_2O$

<i>h</i>	<i>k</i>	<i>l</i>	<i>d</i> _{cal} (Å)	<i>d</i> _{obs} (Å)	<i>I</i> / <i>I</i> ₀	<i>h</i>	<i>k</i>	<i>l</i>	<i>d</i> _{cal} (Å)	<i>d</i> _{obs} (Å)	<i>I</i> / <i>I</i> ₀
1	0	0	9.364	9.365	100	3	1	0	2.972	2.971	83
						3	1	-3	2.964		
0	1	1	8.077	8.077	74						
						1	3	1	2.936	2.937	72
1	0	-2	6.894	6.895	37	1	3	-2	2.933		
1	1	0	6.745	6.742	54	3	0	-4	2.858	2.857	19
1	1	-1	6.735								
						2	2	2	2.821	2.821	44
1	1	1	5.641	5.644	20	4	1	0	2.276	2.272	13
1	1	-2	5.624	5.619	30	3	2	-5	2.274		
1	0	2	5.013	5.022	17	4	2	1	2.007		
						1	3	5	2.005	2.006	13
0	2	0	4.862	4.866	17	4	2	-5	2.001		
2	0	-2	4.669	4.673	20	2	4	2	1.990		
						1	2	6	1.988	1.988	22
0	1	3	4.329			2	2	5	1.986		
1	2	0	4.315	4.319	46						
1	2	-1	4.312			5	1	-4	1.897	1.899	17
						1	0	-8	1.896		
2	1	0	4.218	4.217	39						
						3	4	2	1.771	1.771	15
0	2	2	4.038	4.040	19						
						1	4	-6	1.758	1.759	19
1	0	-4	3.815	3.815	24	2	5	-3	1.755		
2	1	1	3.771	3.774	19	4	4	-2	1.732	1.732	24
						4	0	4	1.731		24
2	2	-1	3.465	3.469	30						
						4	0	-8	1.724	1.724	11
2	0	-4	3.447	3.449	30						
0	1	4	3.398	3.403	37	0	4	6	1.714	1.716	11
						6	0	0	1.561	1.559	9
1	2	3	3.008	3.010	17						

(NH₄)₂Mo₃TeO₁₂ (1). A 2.0 g (1.62 mmol) sample of (NH₄)₆Mo₇O₂₄·4H₂O and 0.3013 g (1.89 mmol) of TeO₂ along with 4.2 mL of water were heated in a Parr acid digestion bomb for 7 days at 225 °C and then cooled to room temperature over a period of 2 days. (NH₄)₂Mo₃TeO₁₂ was obtained as a major phase (1.064 g, 87.5% yield) in the form of bright yellow blocks of crystals, enabling their physical separation (see trial A3 in Table 1).

Cs₂Mo₃TeO₁₂ (2). This compound, as in the case of **1**, was similarly obtained as a major phase (0.925 g, 87% yield) in the form of a bright yellow microcrystalline solid when 0.8 g (2.45 mmol) of Cs₂CO₃, 0.703 g (4.88 mmol) of MoO₃, and 0.195 g (1.22 mmol) of TeO₂ along with 4.4 mL of water were reacted under similar hydrothermal conditions (see trial C2 in Table 1). Single crystals suitable for X-ray diffraction

Table 6. Atomic Coordinates ($\times 10^4$) and Equivalent Isotropic Displacement Parameters ($\text{\AA}^2 \times 10^3$) for (NH₄)₂Mo₃TeO₁₂ (**1**) and Cs₂Mo₃TeO₁₂ (**2**)

atom	<i>x</i>	<i>y</i>	<i>z</i>	<i>U</i> _{eq} ^a
Compound 1				
N(1)	3333	6667	1148(19)	28(5)
N(2)	6667	3333	2341(16)	20(4)
Mo	1327(1)	3408(1)	3909(1)	8(1)
Te	0	0	1473(1)	9(1)
O(1)	2470(12)	1250(11)	4046(10)	14(2)
O(2)	4017(15)	1989(12)	289(7)	15(2)
O(3)	829(12)	5463(11)	3507(7)	8(2)
O(4)	1362(11)	2598(14)	2228(6)	12(2)
Compound 2				
Cs(1)	3333	6667	918(2)	24(1)
Cs(2)	6667	3333	2323(1)	14(1)
Mo	1347(1)	3394(2)	3946(1)	4(1)
Te	0	0	1571(1)	6(1)
O(1)	2517(13)	1250(12)	4105(12)	11(2)
O(2)	3938(16)	1899(15)	312(10)	11(2)
O(3)	899(14)	5450(13)	3566(9)	9(2)
O(4) ^b	1390(15)	2561(16)	2318(9)	11(2)

^a *U*_{eq} is defined as one-third of the trace of the orthogonalized **U**_{ij} tensor. ^b Atom refined isotropically.

studies were obtained when the hydrothermal reaction was carried out in a 45-mL bomb under similar conditions of 225 °C and 6 days with a reactant mixture of 0.75 g (2.30 mmol) of Cs₂CO₃, 0.663 g (4.61 mmol) of MoO₃, 0.184 g (1.15 mmol) of TeO₂, and 8 mL of water.

Compound **2** was prepared as a pure phase in the polycrystalline form by heating a stoichiometric mixture of Cs₂CO₃, MoO₃, and TeO₂ from 400 to 475 °C over a period of 3 days with four intermittent grindings and finally at 475 °C for 15 h.

Rb₄Mo₆Te₂O₂₄·6H₂O (3). A mixture of Rb₂CO₃ (0.412 g, 1.78 mmol), MoO₃ (0.513 g, 3.56 mmol), and TeO₂ (0.285 g, 1.78 mmol) in a 2:2:1 ratio of Rb:Mo:Te was heated hydrothermally with 4.4 mL of water for 4 days and then cooled to room temperature over 2 days. White transparent blocks of crystals of **3** (about 0.35 g) were picked from a mixture of products. The other products were not identified.

This compound was obtained in the pure form as a powder (0.633 g, 70.2% yield) by simple refluxing of a stoichiometric mixture of Rb₂CO₃ (0.25 g, 1.08 mmol), MoO₃ (0.467 g, 3.24 mmol), and TeO₂ (0.173 g, 1.08 mmol) in 30 mL of distilled water for 30 h. The solid product was filtered off, washed with distilled water, and air-dried.

K₄Mo₆Te₂O₂₄·6H₂O (4). This compound was also similarly obtained as white transparent blocks of crystals, along with other unidentified products, by heating hydrothermally a mixture of 0.279 g (2.02 mmol) of K₂CO₃, 0.582 g (4.04 mmol) of MoO₃, and 0.161 g (1.01 mmol) of TeO₂ (K:Mo:Te = 4:4:1) at 225 °C for 6 days and cooling to room temperature over 2 days.

As for the compound **3**, this was also prepared as a pure polycrystalline phase (0.543 g, 58.5% yield) by heating a stoichiometric mixture

Table 5. Crystallographic Data for (NH₄)₂Mo₃TeO₁₂ (**1**), Cs₂Mo₃TeO₁₂ (**2**), Rb₄Mo₆Te₂O₂₄·6H₂O (**3**), and K₄Mo₆Te₂O₂₄·6H₂O (**4**)

	1	2	3	4
empirical formula	N ₂ Mo ₃ TeO ₁₂ H ₈	Cs ₂ Mo ₃ TeO ₁₂	Rb ₄ Mo ₆ Te ₂ O ₃₀ H ₁₂	K ₄ Mo ₆ Te ₂ O ₃₀ H ₁₂
<i>a</i> (Å)	7.332(2)	7.3956(10)	10.0564(14)	9.878(3)
<i>b</i> (Å)			9.877(8)	9.724(4)
<i>c</i> (Å)	12.028(4)	12.186(2)	15.724(3)	15.301(3)
β (deg)			109.988(11)	108.57(2)
<i>V</i> (Å ³)	560.0(3)	577.2(2)	1467.7(12)	1393.0(7)
<i>Z</i>	2	2	2	2
fw	643.50	873.24	1664.82	1479.34
<i>T</i> (°C)	25	25	25	25
space group	<i>P</i> 6 ₃ (No. 173)	<i>P</i> 6 ₃ (No. 173)	<i>P</i> 2 ₁ / <i>c</i> (No. 14)	<i>P</i> 2 ₁ / <i>c</i> (No. 14)
λ (Mo K α) (Å)	0.710 73	0.710 73	0.710 73	0.710 73
ρ _{calcd} (g/cm ³)	3.816	5.024	3.767	3.527
μ (Mo K α) (mm ⁻¹)	5.922	11.958	11.133	5.384
<i>R</i> ^a	0.0273	0.0285	0.0339	0.0303
<i>R</i> _w ^b	0.0637	0.0674	0.0753	0.0746

$$^a R = \sum ||F_o| - |F_c|| / \sum |F_o|. \quad ^b R_w = [\sum w(|F_o|^2 - |F_c|^2)^2 / \sum w|F_o|^2]^{1/2}.$$

Table 7. Selected Bond Lengths (Å) and Angles (deg) for $A_2Mo_3TeO_{12}$ ($A = NH_4, Cs$) Compounds

	$(NH_4)_2Mo_3TeO_{12}$	$Cs_2Mo_3TeO_{12}$
Mo–O(1)	1.772(7)	1.783(8)
Mo–O(1)′	2.135(7)	2.162(8)
Mo–O(2)	1.728(8)	1.729(12)
Mo–O(3)	1.786(7)	1.771(9)
Mo–O(3)′	2.111(7)	2.130(9)
Mo–O(4)	2.112(8)	2.082(11)
Te–O(4) × 3	1.884(9)	1.877(10)
A(1)–O(1) × 3		3.456(12)
A(1)–O(3) × 3	3.25(2)	
A(1)–O(4) × 3	2.892(14)	3.135(10)
A(2)–O(1) × 3	3.362(14)	3.432(11)
A(2)–O(2) × 3	2.99(2)	3.010(11)
A(2)–O(3) × 3	2.992(13)	3.106(10)
O(1)–Mo–O(1)′	87.6(4)	89.6(5)
O(1)′–Mo–O(2)	86.6(4)	84.5(5)
O(1)–Mo–O(2)	100.9(5)	99.4(6)
O(1)′–Mo–O(3)	163.5(4)	165.5(5)
O(1)–Mo–O(3)′	165.5(4)	167.5(4)
O(2)–Mo–O(3)′	87.6(4)	87.0(5)
O(1)′–Mo–O(3)′	78.7(3)	80.4(4)
O(2)–Mo–O(3)	101.7(4)	102.3(5)
O(1)–Mo–O(3)	102.3(4)	101.8(4)
O(3)–Mo–O(3)′	89.6(5)	87.1(5)
O(1)–Mo–O(4)	89.5(4)	90.7(5)
O(1)′–Mo–O(4)	78.5(4)	78.3(5)
O(2)–Mo–O(4)	161.5(3)	160.0(4)
O(3)–Mo–O(4)	90.8(4)	92.4(5)
O(3)′–Mo–O(4)	78.8(3)	80.1(4)
O(4)–Te–O(4)	98.7(3)	98.5(4)
Mo–O(1)–Mo	150.4(5)	147.8(5)
Mo–O(3)–Mo	136.1(4)	139.2(6)
Mo–O(4)–Te	132.2(4)	132.7(5)

Table 8. Atomic Coordinates ($\times 10^4$) and Equivalent Isotropic Displacement Parameters ($\text{Å}^2 \times 10^3$) for $Rb_4Mo_6Te_2O_{24} \cdot 6H_2O$ (3)

atom	x	y	z	U_{eq}^a
Te	5777(1)	1109(1)	9209(1)	12(1)
Mo(1)	2754(1)	2447(1)	9926(1)	15(1)
Mo(2)	8094(1)	−53(1)	1606(1)	16(1)
Mo(3)	5852(1)	2396(1)	1530(1)	15(1)
Rb(1)	2631(1)	1219(1)	2414(1)	28(1)
Rb(2)	9097(1)	1391(1)	5721(1)	32(1)
O(1)	4139(5)	807(5)	885(3)	16(1)
O(2)	3846(5)	1350(5)	9069(3)	16(1)
O(3)	6631(5)	1333(5)	476(3)	16(1)
O(4)	1572(5)	922(5)	9398(3)	17(1)
O(5)	6866(5)	830(5)	2141(3)	19(1)
O(6)	4578(5)	1759(5)	5456(3)	19(1)
O(7)	1995(6)	2182(6)	5724(4)	27(1)
O(8)	2052(6)	1377(5)	4093(3)	25(1)
O(9)	1246(6)	1242(5)	7574(3)	24(1)
O(10)	9406(6)	1126(6)	1806(4)	26(1)
O(11)	7207(6)	1472(6)	6756(4)	24(1)
O(12)	5025(6)	2156(6)	7274(3)	24(1)
O(13)	8600(9)	765(11)	9183(7)	85(3)
O(14)	5931(11)	893(9)	3969(7)	85(3)
O(15)	9086(10)	1326(12)	3857(5)	91(3)

^a U_{eq} is defined as one-third of the trace of the orthogonalized U_{ij} tensor.

of 0.173 g (1.25 mmol) of K_2CO_3 , 0.542 g (3.76 mmol) of MoO_3 , and 0.2 g (1.25 mmol) of TeO_2 under the same refluxing conditions.

X-ray Diffraction and Crystal Structure. The powder X-ray diffraction patterns were recorded on a Rigaku Miniflex (Table model) instrument using $Co\ K\alpha$ radiation ($\lambda = 1.7902\text{ Å}$) and also on a Seifert automated powder diffractometer using $Cu\ K\alpha_1$ radiation (a germanium single crystal was used as a monochromator; $Cu\ K\alpha_1$, $\lambda = 1.5406\text{ Å}$). Silicon was used as an external standard. The monophasic natures of the four compounds were ascertained by comparing their powder X-ray diffraction patterns (Tables 2–4) with those simulated on the

Table 9. Atomic Coordinates ($\times 10^4$) and Equivalent Isotropic Displacement Parameters ($\text{Å}^2 \times 10^3$) for $K_4Mo_6Te_2O_{24} \cdot 6H_2O$ (4)

atom	x	y	z	U_{eq}^a
Te	5807(1)	1135(1)	9191(1)	11(1)
Mo(1)	2680(1)	2442(1)	9900(1)	14(1)
Mo(2)	8075(1)	16(1)	1643(1)	14(1)
Mo(3)	5760(1)	2457(1)	1529(1)	15(1)
K(1)	2505(2)	1298(2)	2384(1)	30(1)
K(2)	9083(2)	1366(2)	5800(1)	39(1)
O(1)	4071(4)	801(4)	890(3)	17(1)
O(2)	3833(4)	1331(4)	9045(3)	14(1)
O(3)	6620(4)	1388(4)	484(2)	14(1)
O(4)	1530(4)	868(4)	9379(3)	17(1)
O(5)	6788(4)	891(4)	2180(2)	17(1)
O(6)	4500(4)	1714(4)	5429(3)	16(1)
O(7)	1871(5)	2203(5)	5711(3)	26(1)
O(8)	1968(5)	1380(4)	4049(3)	23(1)
O(9)	1242(5)	1173(5)	7516(3)	24(1)
O(10)	9394(4)	1230(5)	1835(3)	26(1)
O(11)	7116(5)	1366(4)	6765(3)	26(1)
O(12)	4842(5)	2116(5)	7270(3)	25(1)
O(13)	8633(8)	855(15)	9079(8)	143(5)
O(14)	5875(15)	922(7)	3908(7)	129(5)
O(15) ^b	8981(12)	1049(15)	4049(7)	128(7)

^a U_{eq} is defined as one-third of the trace of the orthogonalized U_{ij} tensor. ^b Site occupancy is 0.90(3).

basis of their single-crystal X-ray structure using the LAZY-PULVERIX program.¹¹ The cell parameters of **1** and **2**, obtained from their powder X-ray diffraction patterns, were refined using the AUTOX program.¹²

Single crystals of the compounds **1–4**, suitable for X-ray diffraction, were selected from the products of hydrothermal reactions. They were mounted on thin glass fibers with epoxy glue. Data sets were gathered from the crystals on a Rigaku AFC7 automated diffractometer for compound **1** and on an Enraf-Nonius CAD4 automated four-circle diffractometer for the other three compounds by standard procedures. Pertinent crystallographic data and data collection parameters are summarized in Table 5. About 20 reflections with $14^\circ \leq 2\theta \leq 35^\circ$ were located and centered. Their least-squares refinement resulted in hexagonal unit cells for **1** and **2** and monoclinic unit cells for **3** and **4**. The data sets from all the crystals were reduced by routine computational procedures. Absorption corrections based on azimuthal scans of reflections with a χ angle near 90° were applied to the data sets. Intensities of two or three check reflections monitored at regular intervals remained invariant, indicating no sign of decay or decomposition in all cases. The programs SHELXS-86 and SHELXL-93 were used for structure solutions and structure refinement, respectively.¹³ The positions of metal atoms were located by direct methods. Refinement of these positions and subsequent difference Fourier maps led to the location of the remaining non-hydrogen atoms, namely, nitrogen and oxygen atoms of the asymmetric unit.

For compounds **1** and **2**, the Laue group $6/m$, as adjudged from test data merging, and the only observed systematic absence condition ($00l$, $l = \text{odd}$), indicated the space group to be either noncentrosymmetric $P6_3$ or centrosymmetric $P6_3/m$. The close resemblance of these hexagonal lattice parameters to those of the corresponding selenites⁶ indicated the possible similarity between tellurites and selenites, and hence, the same noncentrosymmetric $P6_3$ space group of selenites was chosen. This was later proved to be correct by successful refinement and also by nonzero second-harmonic-generation response as indicated by the green emission at 532 nm upon exposure to the fundamental line, at 1064 nm, of a Q-switched Nd:YAG laser (Quanta-Ray). The structures were found to be isostructural with their corresponding selenites. Anisotropic refinement of all the atoms proceeded smoothly

- (11) Yvon, K.; Jeitschko, W.; Parthe, E. *J. Appl. Crystallogr.* **1977**, *10*, 73.
 (12) Zlokazov, V. B. *J. Appl. Crystallogr.* **1992**, *25*, 69.
 (13) (a) Sheldrick, G. M. SHELXS-86 User Guide. Crystallography Department, University of Gottingen, Germany, 1985. (b) Sheldrick, G. M. SHELXL-93 User Guide. Crystallography Department, University of Gottingen, Germany, 1993.

Table 10. Selected Bond Lengths (Å) and Angles (deg) for $A_4Mo_6Te_2O_{24} \cdot 6H_2O$ (A = Rb, K) Compounds

	A = Rb	A = K		A = Rb	A = K
Mo(1)—O(1)	2.324(5)	2.325(4)	Te—O(3)	1.894(5)	1.901(4)
Mo(1)—O(2)	2.282(5)	2.263(4)	A(1)—O(1)	3.278(5)	3.178(4)
Mo(1)—O(4)	1.923(5)	1.921(4)	A(1)—O(2)	3.442(5)	3.372(4)
Mo(1)—O(6)	1.905(5)	1.906(4)	A(1)—O(7)	2.967(6)	2.836(5)
Mo(1)—O(7)	1.716(5)	1.712(4)	A(1)—O(8)	2.895(5)	2.764(5)
Mo(1)—O(8)	1.712(5)	1.709(4)	A(1)—O(9)	2.921(6)	2.794(5)
Mo(2)—O(2)	2.272(5)	2.261(4)	A(1)—O(10)	3.053(5)	2.917(5)
Mo(2)—O(3)	2.325(5)	2.317(4)	A(1)—O(11)	2.941(6)	2.870(5)
Mo(2)—O(4)	1.925(5)	1.930(4)	A(1)—O(12)	2.964(6)	2.827(5)
Mo(2)—O(5)	1.925(5)	1.918(4)	A(1)—O(13)	3.091(10)	3.009(12)
Mo(2)—O(9)	1.702(5)	1.701(4)	A(1)—O(14)	3.398(10)	3.422(14)
Mo(2)—O(10)	1.706(5)	1.713(4)	A(2)—O(3)	3.271(5)	3.189(4)
Mo(3)—O(1)	2.294(5)	2.300(4)	A(2)—O(7)	3.016(5)	2.917(5)
Mo(3)—O(3)	2.314(5)	2.285(4)	A(2)—O(8)	3.021(6)	2.900(5)
Mo(3)—O(5)	1.920(5)	1.923(4)	A(2)—O(9)	2.979(5)	2.812(4)
Mo(3)—O(6)	1.926(5)	1.923(4)	A(2)—O(10)	2.943(6)	2.785(5)
Mo(3)—O(11)	1.704(5)	1.711(4)	A(2)—O(11)	2.895(5)	2.789(5)
Mo(3)—O(12)	1.709(5)	1.714(4)	A(2)—O(14)	3.460(10)	
Te—O(1)	1.902(5)	1.893(4)	A(2)—O(15)	3.186(11)	2.991(13)
Te—O(2)	1.893(5)	1.901(4)	A(2)—O(15)	2.929(8)	2.667(10)

	A = Rb	A = K		A = Rb	A = K
O(2)—Mo(1)—O(1)	75.5(2)	75.37(14)	O(3)—Mo(3)—O(1)	76.1(2)	76.44(14)
O(4)—Mo(1)—O(1)	83.1(2)	82.7(2)	O(5)—Mo(3)—O(1)	82.0(2)	81.8(2)
O(4)—Mo(1)—O(2)	74.0(2)	73.7(2)	O(5)—Mo(3)—O(3)	75.0(2)	75.5(2)
O(6)—Mo(1)—O(1)	74.3(2)	74.8(2)	O(5)—Mo(3)—O(6)	150.3(2)	150.8(2)
O(6)—Mo(1)—O(2)	82.4(2)	82.6(2)	O(6)—Mo(3)—O(1)	74.6(2)	75.1(2)
O(6)—Mo(1)—O(4)	150.7(2)	150.7(2)	O(6)—Mo(3)—O(3)	81.7(2)	81.9(2)
O(7)—Mo(1)—O(1)	89.6(2)	88.9(2)	O(11)—Mo(3)—O(1)	165.3(2)	166.2(2)
O(7)—Mo(1)—O(2)	163.2(2)	162.2(2)	O(11)—Mo(3)—O(3)	90.3(2)	90.6(2)
O(7)—Mo(1)—O(4)	96.8(2)	96.4(2)	O(11)—Mo(3)—O(5)	100.0(2)	99.9(2)
O(7)—Mo(1)—O(6)	101.2(2)	101.5(2)	O(11)—Mo(3)—O(6)	98.2(2)	98.6(2)
O(8)—Mo(1)—O(1)	165.5(2)	166.3(2)	O(11)—Mo(3)—O(12)	103.2(3)	104.0(2)
O(8)—Mo(1)—O(2)	91.5(2)	92.3(2)	O(12)—Mo(3)—O(1)	90.7(2)	89.2(2)
O(8)—Mo(1)—O(4)	99.7(2)	99.9(2)	O(12)—Mo(3)—O(3)	166.2(2)	165.1(2)
O(8)—Mo(1)—O(6)	98.0(2)	97.9(2)	O(12)—Mo(3)—O(5)	99.5(2)	98.8(2)
O(8)—Mo(1)—O(7)	104.2(3)	104.1(2)	O(12)—Mo(3)—O(6)	98.9(2)	98.4(2)
O(2)—Mo(2)—O(3)	75.9(2)	75.84(14)	O(1)—Te—O(2)	100.8(2)	100.2(2)
O(4)—Mo(2)—O(2)	74.2(2)	73.6(2)	O(1)—Te—O(3)	100.5(2)	100.5(2)
O(4)—Mo(2)—O(3)	83.0(2)	82.7(2)	O(2)—Te—O(3)	100.7(2)	100.7(2)
O(5)—Mo(2)—O(2)	83.3(2)	83.6(2)	Mo(1)—O(4)—Mo(2)	116.6(2)	116.4(2)
O(5)—Mo(2)—O(3)	74.6(2)	74.8(2)	Mo(1)—O(6)—Mo(3)	117.3(3)	116.8(2)
O(5)—Mo(2)—O(4)	151.5(2)	151.3(2)	Mo(2)—O(2)—Mo(1)	91.9(2)	92.71(14)
O(9)—Mo(2)—O(2)	90.8(2)	91.7(2)	Mo(2)—O(5)—Mo(3)	117.2(2)	116.3(2)
O(9)—Mo(2)—O(3)	165.0(2)	166.0(2)	Mo(3)—O(1)—Mo(1)	90.2(2)	89.7(2)
O(9)—Mo(2)—O(4)	100.4(2)	100.2(2)	Mo(3)—O(3)—Mo(2)	90.0(2)	90.28(13)
O(9)—Mo(2)—O(5)	97.1(2)	97.8(2)	Te—O(1)—Mo(1)	132.5(2)	132.6(2)
O(9)—Mo(2)—O(10)	104.8(3)	104.0(2)	Te—O(2)—Mo(1)	132.3(2)	131.8(2)
O(10)—Mo(2)—O(2)	163.3(2)	162.7(2)	Te—O(2)—Mo(2)	131.8(2)	131.9(2)
O(10)—Mo(2)—O(3)	89.2(2)	89.2(2)	Te—O(3)—Mo(2)	132.6(2)	132.5(2)
O(10)—Mo(2)—O(4)	96.6(2)	96.1(2)	Te—O(1)—Mo(3)	131.9(2)	132.2(2)
O(10)—Mo(2)—O(5)	100.5(2)	101.1(2)	Te—O(3)—Mo(3)	131.6(2)	131.3(2)

for **1**. For **2**, on the other hand, one oxygen atom, namely O(4), became nonpositive definite and hence O(4) alone was refined isotropically in the final cycles of refinement.

For compounds **3** and **4**, the space groups $P2_1/n$ and $P2_1/c$ were unambiguously determined from the systematic absences of the observed data. As these two compounds turned out to be isostructural, the original monoclinic unit cell with the space group $P2_1/n$ of compound **3** was transformed to the new monoclinic unit cell with the space group $P2_1/c$. One tellurium, crystallographically distinct three molybdenums, two alkali metals, and fifteen oxygen atoms were found to be present in the asymmetric unit. While the three oxygen atoms O(13)—O(15) represent the water of crystallization, the remaining twelve of them, along with molybdenum and tellurium atoms, constitute only a half of the $(Mo_6Te_2O_{24})^{4-}$ anion and the halves are related by a crystallographic inversion center. All atoms were refined anisotropically. The thermal parameters of oxygen atoms of water molecules were found to be large and indicated the possibility of their partial site occupancy. This led us to vary their site occupancies in the subsequent refinements for both **3** and **4**. For compound **3**, no change was observed

from the value of 1 for those site occupancy factors. These occupancies were, therefore, not refined in the later cycles. In the final refinement, a total of 190 parameters were refined with a data-to-parameter ratio of 13.54. For compound **4**, on the other hand, the site occupancy of only one oxygen atom, namely O(15), decreased to about 0.9. In the final cycles of refinement, a total of 191 parameters, including the site occupancy of O(15), were refined and the data-to-parameter ratio was 12.88. There was a marginal improvement in the thermal parameters of O(13)—O(15) and the values of R and R_w . These compounds are, hereafter, referred to by idealized compositions, $A_4Mo_6Te_2O_{24} \cdot 6H_2O$ (A = Rb, K).

Thermal Studies. Thermogravimetric analytical (TGA) and differential scanning calorimetric (DSC) data were collected on a Perkin-Elmer Delta Series TG instrument. Some of the TGA data were collected on a Dupont 2000 Thermal Analyst. The samples of **1** and **2** were heated to about 1000 °C at a rate of 10 °C/min whereas compounds **3** and **4** were heated to about 600 °C at a rate of 20 °C/min under flowing N_2 gas.

Spectroscopic Data. The samples were ground with dry KBr and pressed into transparent disks. The infrared spectra was measured on these transparent disks from 400 to 4000 cm^{-1} , for all four samples on a Bruker 17S, 66V FT-IR spectrometer. Raman spectra were recorded on an RFS 100 FT Raman spectrometer with an FRA 106 FT-Raman accessory provided with a CaF_2 beam splitter. An Nd:YAG laser operating at an output of 200 mW for a 1064 nm line was used as the excitation source.

Results and Discussion

Syntheses. We carried out a number of hydrothermal synthetic experiments, some of which are listed in Table 1, by varying three parameters, namely, ratio of reactants and duration and temperature of heating, and finally arrived at the optimum conditions, as given in the Experimental Section for the title compounds. TeO_2 , unlike SeO_2 , is insoluble in water. However, it dissolved in the solutions as the reactions proceeded. The final pH in all these reactions was neutral. Our initial trials, A1 and C1, were patterned after the reported synthesis of selenite analogues.⁶

The first trial, A1, yielded a mixture of new solid products including the required compound **1**, $(\text{NH}_4)_2\text{Mo}_3\text{TeO}_{12}$, as a few bright yellow chunky crystals. The other two solid products were colorless plates of hexagonal phase with a 1:1 ratio of Mo:Te and white needlelike crystals of $(\text{NH}_4)_4\text{Mo}_6\text{TeO}_{22}\cdot 2\text{H}_2\text{O}$, which will be reported elsewhere. Under the same reaction conditions, the use of seed crystals improved the yield of compound **1**. A change of ratio of Mo:Te to 6:1 in the reactant mixture (trial A3) eliminated the formation of the hexagonal phase and gave only a biphasic mixture of the other two products, the yield of title compound being 87.5%. Attempts using a higher reaction temperature of 235 °C for a prolonged period of 14 days (trial A4) led to only slight improvement in the yield. The title compound, however, could not be prepared when lower temperatures and shorter durations, for example as in trial A5, were used. Even the best standardized conditions (trial A3) could yield this compound as only the major phase of a biphasic product mixture.

Compound **2**, $\text{Cs}_2\text{Mo}_3\text{TeO}_{12}$, unlike its selenium analogue, could not be synthesized from a stoichiometric mixture of reactants as in trial C1. It could only be prepared as the major phase (yield 87%) along with a very small amount of white solid of unidentified composition, when the reactants in a 4:4:1 ratio of Cs:Mo:Te were used (trial C2). The formation of white solid could not be suppressed by using higher temperatures, longer durations, and different ratios of reactants. Our several trials have shown that the yield of compound **2** and even its formation were affected by the other ratios of reactants.

Hydrothermal attempts for layered tellurite analogues of potassium and rubidium failed. Such attempts surprisingly resulted in the entirely new "zero-dimensional" compounds $\text{Rb}_4\text{Mo}_6\text{Te}_2\text{O}_{24}\cdot 6\text{H}_2\text{O}$ (**3**) and $\text{K}_4\text{Mo}_6\text{Te}_2\text{O}_{24}\cdot 6\text{H}_2\text{O}$ (**4**) in multiphasic product mixtures. Our hydrothermal attempts to obtain **3** and **4** in pure form were not successful.

To verify the need for hydrothermal conditions for the synthesis of compounds **1** to **4**, we attempted their synthesis by simple refluxing of an aqueous mixture of reactants. Compounds **3** and **4**, containing water of crystallization, could indeed be prepared as pure polycrystalline samples by this simple method of refluxing a stoichiometric mixture of reactants in water. This procedure gives the same result even when excess alkali metal molybdates are used. A similar procedure for the cesium compound **2** led to the isolation of a polycrystalline sample whose powder pattern is similar to that of $(\text{NH}_4)_4\text{Mo}_6\text{-}$

$\text{TeO}_{22}\cdot 2\text{H}_2\text{O}$. On the other hand, TeO_2 was the only solid recovered in a similar synthetic attempt for the ammonium compound.

We have learned from the thermal investigations that compound **2** is stable even at 500 °C. Thus it has become possible to prepare it in pure form, as a polycrystalline sample, by the solid-state reaction of a stoichiometric mixture of $\text{Cs}_2\text{-CO}_3$, MoO_3 , and TeO_2 at temperatures as low as 475 °C. However, the potassium and rubidium analogues of layered tellurites could not be prepared by similar solid-state synthesis. Thus, the pure phases of layered tellurite **2** and "zero-dimensional" tellurites **3** and **4** could be prepared by solid-state reactions and simple refluxing procedures, respectively. Hydrothermal conditions are, therefore, necessary for the synthesis of **1** only.

We have refluxed and/or stirred compound **1** with aqueous solutions of the potassium/rubidium salts KCl, KOH, KNO_3 , RbCl, and RbNO_3 to prepare layered tellurites of potassium and rubidium by ion-exchange reactions. Such attempts have not been successful, and in some of these attempts, partial formation of compound **4** has been observed. A limited number of similar trials carried out with **2** have also failed. NH_4^+ and Cs^+ ions in the layered tellurites are thus immobile under these conditions.

Crystal Structures. The final refined positional and equivalent isotropic thermal parameters for **1** and **2** are given in Table 6. The selected bond lengths and angles are presented in Table 7. Final atomic positional and equivalent isotropic thermal parameters for compounds **3** and **4** are listed in Tables 8 and 9, respectively, with selected bond lengths and angles in Table 10.

Compounds 1 and 2. The two new tellurites, **1** and **2**, and the reported⁶ selenite analogues are all isostructural layered compounds. The tellurites **1** and **2** consist of $(\text{Mo}_3\text{TeO}_{12})^{2-}$ layers in the *ab* plane of the hexagonal cell and $\text{NH}_4^+/\text{Cs}^+$ cations between the layers for charge compensation. The anionic layer can be conceived as consisting of a two-dimensional hexagonal tungsten oxide (HTO)-like sheet of composition MoO_4 or Mo_3O_{12} , formed from sharing of four corners of every MoO_6 octahedron with four such octahedra. Two trans corners of every MoO_6 octahedron are not involved in this type of sharing. Such in-plane connectivity leads to three- and six-ring holes in the layer. Half of these three-ring holes are capped, on only one side, by tellurium to give a very asymmetric two-dimensional $(\text{Mo}_3\text{TeO}_{12})^{2-}$ layer as shown in Figure 1. These layers are stacked, as shown in Figure 1b,c, along the crystallographic *c* axis in the ABAB... fashion because adjacent layers are rotated in the [110] plane with respect to each other such that the six-ring hole of one layer is above the uncapped three-ring hole of its next layer. Therefore pseudo-one-dimensional hexagonal channels, similar to those found in hexagonal WO_3 , are not possible in this structure.

The coordinations of molybdenum, tellurium, and two crystallographically independent cesium/nitrogen atoms with the proper atom-labeling scheme are represented by ORTEP plots¹⁴ in Figures 2 and 3. The molybdenum is octahedrally coordinated to two O(1), two O(3), and two apical oxygen atoms, O(2) and O(4). All these six oxygen atoms form a regular octahedron around molybdenum with maximum, minimum, and average O...O nonbonding distances being 2.785, 2.667, and 2.716 Å for **1** and 2.792, 2.635, and 2.723 Å for **2**. The MoO_6 octahedron is distorted in the sense that the molybdenum is displaced from its geometric center, by 0.33 Å in **1** and 0.32 Å

(14) Johnson, C. K. ORTEP; Oak Ridge National Laboratory: Oak Ridge, TN, 1970.

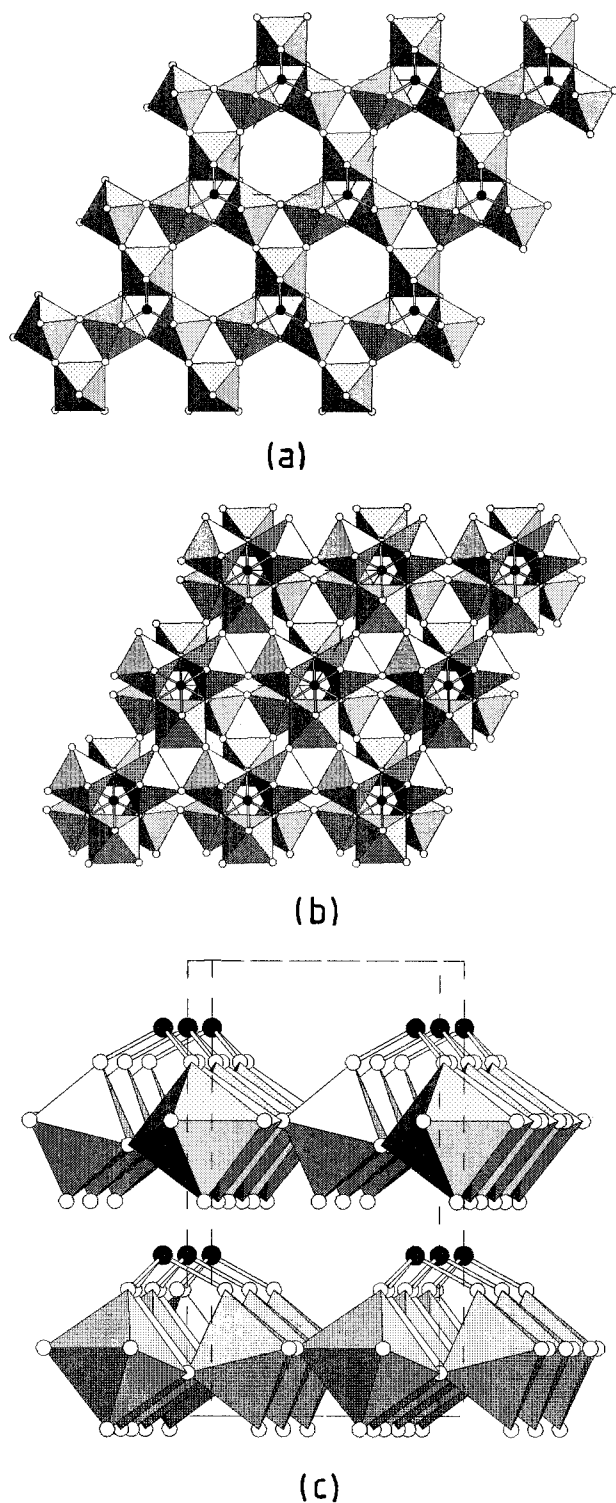


Figure 1. Polyhedral representations of $(\text{Mo}_3\text{TeO}_{12})^{2-}$ layers: (a) single layer viewed along [001]; (b) stacking of two layers viewed along [001]; (c) stacking of two layers viewed along approximately [010].

in **2**, toward one O(1)–O(2)–O(3) triangular face, resulting in three short (<1.79 Å) and three long (>2.08 Å) bonds (Table 7). The short bonds are trans to longer ones. The oxygen O(2) is a terminal oxygen atom bonded to only one metal, namely molybdenum, with a short molybanyl Mo–O bond length of ~ 1.73 Å.

O(1) and O(3) are involved in in-plane connectivity of MoO_6 octahedra, as noted earlier, to give an Mo_3O_{12} HTO-like sheet. This sheet has two types of three-ring holes made of exclusively of either O(1) or O(3) and six-ring holes made of alternating

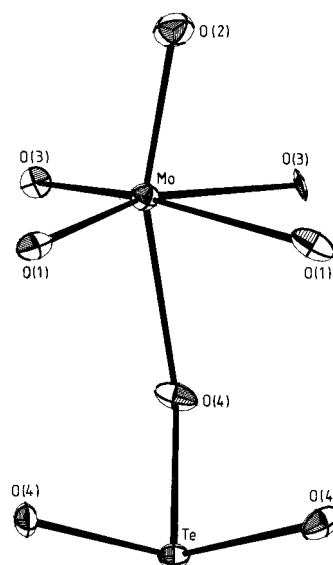


Figure 2. ORTEP view of the Mo/Te/O asymmetric unit of the compounds $(\text{NH}_4)_2\text{Mo}_3\text{TeO}_{12}$ and $\text{Cs}_2\text{Mo}_3\text{TeO}_{12}$, showing the atom-labeling scheme.

O(1) and O(3). Only three-ring holes of O(1) are capped, on one side of the sheet, by bonding of tellurium to apical O(4) oxygen atoms, which just project into the interlayer region. All these features are similar to those found in selenites.⁶

Tellurium sits on a 3-fold axis and has a pyramidal coordination of C_{3v} symmetry, with three equivalent Te–O(4) bonds. The bond lengths and bond angles of the TeO_3 moiety (Table 7) compare well with those in the literature.^{15,16} The bond valence sum calculation¹⁷ for molybdenum and tellurium has given the values of 6.14 and 3.86 for compound **1** and 6.13 and 3.93 for compound **2**, respectively, and these values are closer to the expected values of 6.00 for molybdenum and 4.00 for tellurium.

The crystallographically distinct cations A(1) and A(2) in the interlayer region sit on 3-fold axes and are flanked by an uncapped three-ring hole of one layer and a six-ring hole of the other layer. Thus both A(1) and A(2) could be considered as being surrounded by eighteen oxygen atoms of a polyhedron of the type shown in Figure 3. However, all the eighteen oxygen atoms are not within bonding distances, and thus A(1) and A(2) have six- and nine-coordinations, respectively. N(1) is coordinated to six oxygen atoms, all within distances of 3.5 Å, lying on only one side. These distances suggest that the ammonium ion, $\text{N}(1)\text{H}_4$, is hydrogen-bonded to oxygen atoms of only one layer and not with the oxygen atoms of the other layer. Cs(1), on the other hand, has trigonal prismatic coordination by bonding to three O(4) apical oxygen atoms of one layer and three O(1) oxygen atoms of the six-ring hole in the other layer. N(2) and Cs(2) have nine-coordinations by bonding to three O(2) oxygen atoms of one layer and six oxygen atoms of the six-ring hole of the other layer. Thus N(1), unlike the other three, is not involved in trans layer connections. The hydrogen-bonding in compound **1** is probably similar to that found in the selenite $(\text{NH}_4)_2\text{W}_3\text{SeO}_{12}$.⁷

Compounds 3 and 4. The isostructural compounds $\text{Rb}_4\text{Mo}_6\text{Te}_2\text{O}_{24}\cdot 6\text{H}_2\text{O}$ (**3**) and $\text{K}_4\text{Mo}_6\text{Te}_2\text{O}_{24}\cdot 6\text{H}_2\text{O}$ (**4**) have the so-called “zero-dimensional” structures¹⁰ containing discrete hexamolyb-

(15) Andersen, L.; Langer, V.; Stromberg, A.; Stromberg, D. *Acta Crystallogr.* **1989**, *B45*, 344.

(16) Loopstra, B. O.; Goubitz, K. *Acta Crystallogr.* **1986**, *C42*, 520.

(17) Brese, N. E.; O’Keefe, M. *Acta Crystallogr.* **1991**, *B47*, 192.

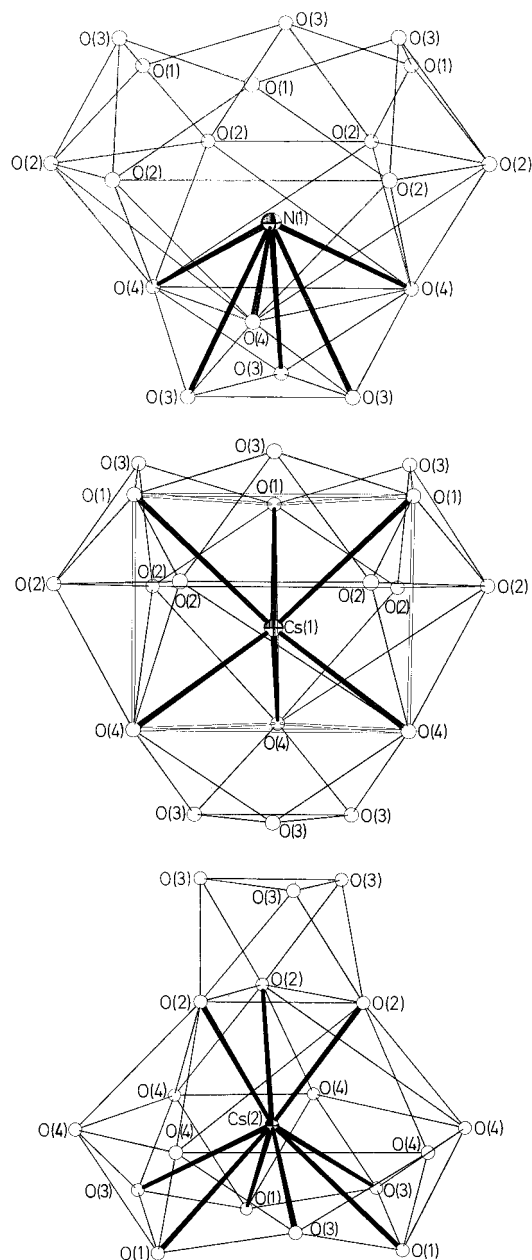


Figure 3. ORTEP views of coordinations of N(1), Cs(1), and Cs(2) in an environment of 18 oxygen atom polyhedra in the compounds $(\text{NH}_4)_2\text{Mo}_3\text{TeO}_{12}$ and $\text{Cs}_2\text{Mo}_3\text{TeO}_{12}$. The nonbonding $\text{O}\cdots\text{O}$ edges of the polyhedra are indicated by thin lines, and oxygen atoms are represented by spheres of arbitrary radius.

doditellurite anionic aggregates $(\text{Mo}_6\text{Te}_2\text{O}_{24})^{4-}$ and cations Rb^+/K^+ . The anion has the same empirical formula of the layered $(\text{Mo}_3\text{TeO}_{12})^{2-}$ anion of compounds **1** and **2**. To the best of our knowledge, the corresponding selenite analogues of compounds **3** and **4** are not known.

The $(\text{Mo}_6\text{Te}_2\text{O}_{24})^{4-}$ anion, as shown in Figures 4 and 5, contains six MoO_6 octahedra and two pyramidal TeO_3 polyhedra, all fused together through corner and edge sharing. Each octahedron shares two edges with two such octahedra to form a nearly flat hexagonal Mo_6O_{24} ring with an octahedral cavity/hole at its center. The two trans open triangular faces of this octahedral hole are capped by tellurium, resulting in pyramidal TeO_3 groups on either side of the hexagonal Mo_6O_{24} ring. The anion could thus be considered as a tellurium-bicapped Mo_6O_{24} hexagonal ring. These anions with idealized symmetry of D_{3d} sit on inversion centers at 2b positions in the unit cell (Figure

4). The cations and water of crystallization (or lattice water) occupy the rest of the lattice.

There are twelve oxygen atoms, O(1)–O(12), for this centrosymmetric anion in the asymmetric unit of the unit cell. As shown in Figure 5, the twenty-four oxygen atoms of the Mo_6O_{24} ring could be derived from two centrosymmetrically related sheets, each sheet composed of these twelve oxygen atoms, O(1)–O(12). The maximum deviation of oxygen atoms from such sheets is 0.197 Å. These two sheets are positioned one over the other in a close-packing fashion. The three molybdenum atoms, Mo(1)–Mo(3), and their inversion-symmetry-related atoms lie near the centers of six octahedra formed between two such sheets, and thus, such an arrangement results in a flat Mo_6O_{24} ring. The six molybdenum atoms of the ring form a perfect plane hexagon around the inversion center, the maximum deviation from the plane being 0.006 Å. The oxygen atoms O(1)–O(12) could be divided into three types. The type a oxygen atoms O(1)–O(3) are each bonded to two molybdenum atoms and one tellurium whereas the type b oxygen atoms O(4)–O(6) are bridging ones, each connected to two molybdenum atoms. The type c oxygen atoms O(7)–O(12) are all terminal ones distributed equally among the three molybdenum atoms, Mo(1)–Mo(3).

The MoO_6 octahedra are all distorted. The values of Mo–O bond lengths vary widely from 1.701 to 2.325 Å, and O–Mo–O bond angles deviate from the ideal values of 90° by as much as 16° (Table 10). The values of Mo–O bond lengths decrease from the Mo–O(a) to the Mo–O(b) to the Mo–O(c) type. The molybdyl Mo–O(c) bonds are trans to long Mo–O(a) bonds. The edges of these octahedra, namely $\text{O}\cdots\text{O}$ nonbonding distances, vary from 2.526 to 2.890 Å. The three shared edges, namely O(1)⋯O(6), O(2)⋯O(4), and O(3)⋯O(5), are 2.526–2.596 Å long and shorter than the other edges by approximately 0.1 Å. The six molybdenum atoms are in fact displaced from the centers of the octahedra by about 0.41 Å toward the type c terminal oxygen atoms. This kind of distortion with such Mo–O bond length variations indicates the stretching of the flat hexagonal Mo_6O_{24} ring radially outward from its center in order to minimize the mutual repulsion between Mo^{6+} ions. This type of flat hexagonal Mo_6O_{24} ring with similar distortions has been reported for many ions,^{18–21} such as $[\text{Mo}_6(\text{CH}_3\text{As})_2\text{O}_{24}]^{4-}$ and $(\text{Mo}_6\text{TeO}_{24})^{6-}$. In the former case, the octahedral cavity is occupied by CH_3As groups, whereas in the latter, it is actually filled by Te^{6+} .

Tellurium is pyramidally coordinated to three type a oxygen atoms with Te–O bond lengths of 1.893–1.902 Å and O–Te–O bond angles of ~100.5°. The values of Te–O bond lengths indicate that the TeO_3^{2-} groups are of the pyramidal MXY_2 type. While the values of these bond angles are comparable to those of pyramidal TeO_3 in alkali metal tellurites^{15,16} such as K_2TeO_3 , the Te–O bonds are definitely longer. Also, these dimensions are greater than those observed in the layered tellurites, **1** and **2**. Furthermore, the edge length of the oxygen triangular base of pyramidal TeO_3 in these compounds is 2.92 Å, which is considerably longer than 2.85 Å observed in compounds **1** and **2**, and the distances of tellurium from this oxygen triangular base are 0.909 Å in compounds **1** and **2** and

- (18) (a) Kwak, W.; Rajkovic, L. M.; Stalick, J. K.; Pope, M. T.; Quicksall, C. O. *Inorg. Chem.* **1976**, *15*, 2778. (b) Kobayashi, A.; Yagasaki, A. *Inorg. Chem.* **1997**, *36*, 126.
 (19) Evans, H. T., Jr. *Acta Crystallogr.* **1974**, *B30*, 2095.
 (20) Fuchs, B. J.; Hart, H. *Angew. Chem., Int. Ed. Engl.* **1976**, *15*, 375.
 (21) (a) Robl, C.; Frost, M. *Z. Naturforsch.* **1993**, *B48*, 404. (b) Robl, C.; Frost, M. *Z. Anorg. Allg. Chem.* **1993**, *619*, 1132. (c) Robl, C.; Frost, M. *Z. Anorg. Allg. Chem.* **1993**, *619*, 1137.

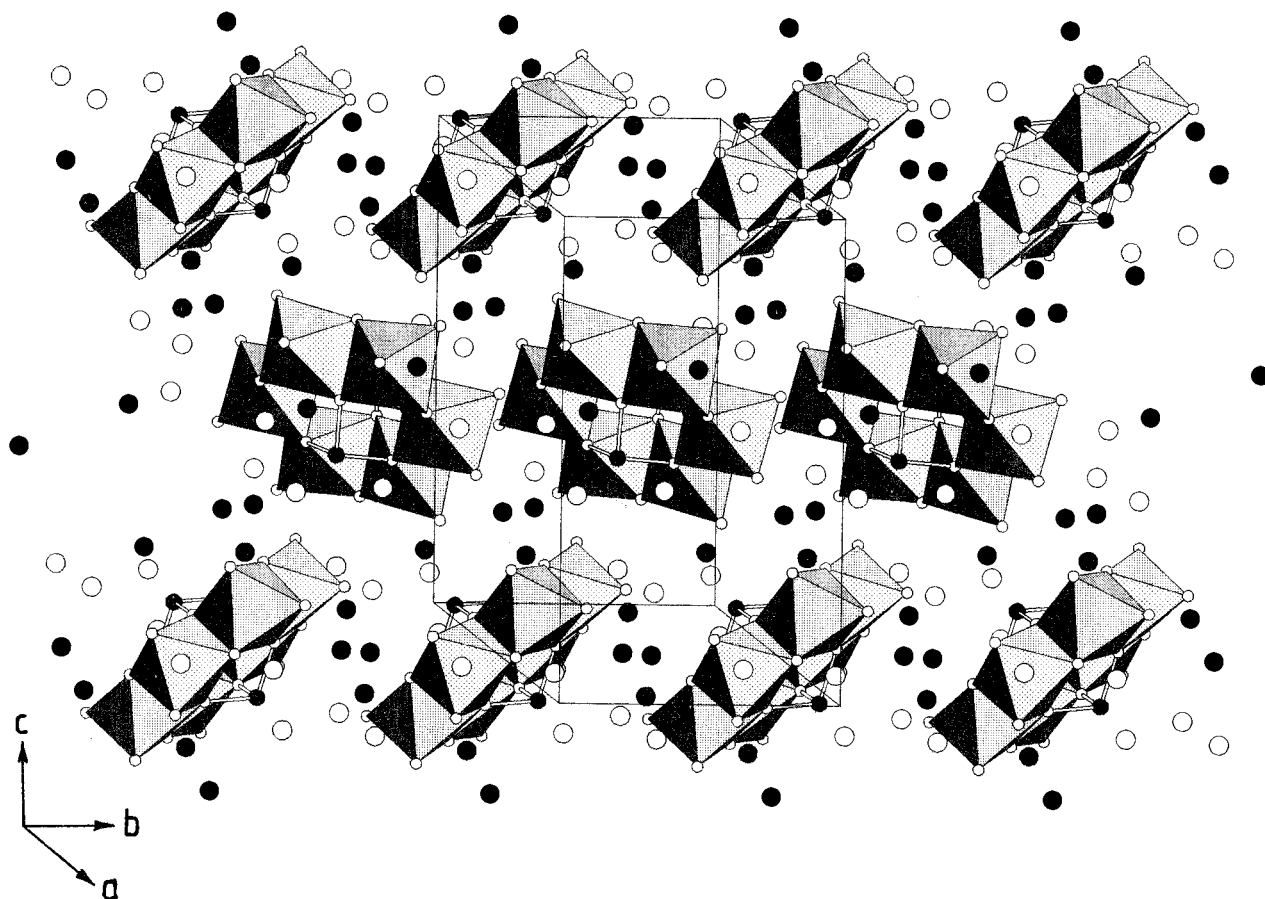


Figure 4. Unit cell diagram of $K_4Mo_6Te_2O_{24} \cdot 6H_2O$ with the polyhedral representation of the $(Mo_6Te_2O_{24})^{4-}$ anion. All atoms are represented by spheres of arbitrary radii. Isolated filled and empty spheres represent potassium atoms and oxygen atoms of water molecules, respectively.

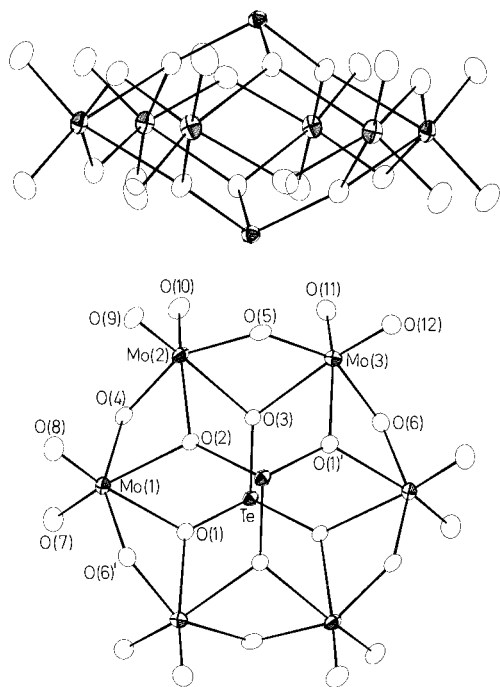


Figure 5. ORTEP views of the $(Mo_6Te_2O_{24})^{4-}$ anion viewed perpendicular to the 3-fold axis (top) and approximately along the 3-fold axis (bottom), showing the atom-labeling scheme.

0.87 Å in compounds **3** and **4**. These values indicate that the TeO_3 moiety is flattened more in the compounds **3** and **4** than in the compounds **1** and **2**. The dimensions of the $(Mo_6Te_2O_{24})^{4-}$ anion do not seem to vary with the size of countercation,

potassium or rubidium. The bond valence sum calculations for tellurium in compounds **3** and **4** gave values of 3.73 and 3.71, respectively. For molybdenum in both compounds, the values lie in the range 6.01–6.07, which are in good agreement with the expected value of 6.00.

There are two crystallographically distinct alkali metal ions, A(1) and A(2), which are coordinated to oxygen atoms of water molecules as well as type a and type c oxygen atoms as shown in Figure 6. Both K(1) and Rb(1) are ten-coordinated with similar geometries. K(2) is eight coordinated, while Rb(2) is nine-coordinated. The Rb(2)–O₉ polyhedron is similar to the K(2)–O₈ polyhedron, but with one more oxygen atom, namely O(14) at 3.460 Å from rubidium.

There seems to be some hydrogen-bonding interaction²² of the water molecules in the lattice. The shortest nonbonding O···O distances between water molecules for compounds **3** and **4** are respectively 2.988 and 3.001 Å, which are indicative of weak hydrogen-bonding between them. Stronger hydrogen-bonding exists between the water molecules and the oxygen atoms of the molecular anion, because some of these O···O nonbonding distances are as short as 2.837 and 2.822 Å in compounds **3** and **4**.

Thermal Studies. Thermogravimetric analysis of compound **1** has shown that it undergoes initially a weight loss of 10.3% at about 390 °C and further weight loss at about 710 °C (Figure 7). The endothermic peak at 390 °C observed in its DSC measurement corresponds to the first weight loss. We heated

(22) (a) Hamilton, W. C.; Ibers, J. A. *Hydrogen Bonding in Solids: Methods of Molecular Structure Determination*; W. A. Benjamin, Inc: New York, 1968. (b) Chippindale, A. M.; Brech, S. J. *J. Chem. Soc., Chem. Commun.* **1996**, 2781.

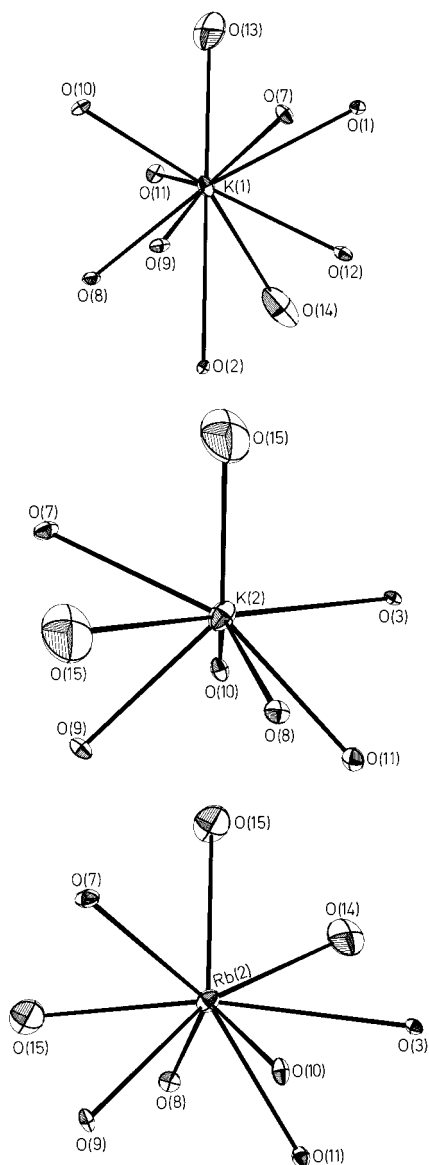


Figure 6. ORTEP views of the coordinations of K(1), K(2), and Rb(2) in the compounds $K_4Mo_6Te_2O_{24} \cdot 6H_2O$ and $Rb_4Mo_6Te_2O_{24} \cdot 6H_2O$.

a bulk sample of compound **1** in a furnace under flowing N_2 atmosphere at $400^\circ C$. A 10.7% weight loss was observed, and the dark blue-black product of the first stage decomposition, as adjudged from its powder X-ray diffraction pattern, contains mostly the Mo_5TeO_{16} phase.²³ The first stage of decomposition involves the loss of NH_3 and H_2O , and the second stage of decomposition is probably due to the loss of volatile component oxides.

Compound **2**, on the other hand, showed no weight loss until $740^\circ C$ (Figure 7). The weight loss starting from $740^\circ C$ should only be due to loss of component oxides. The only endothermic peak observed at $500^\circ C$ in the DSC measurement corresponds to its melting as verified by heating the bulk samples in flowing N_2 gas separately. Surprisingly, the compound retains its structure even on melting, as indicated by the powder X-ray diffraction pattern of the solidified melt.

It is evident from the thermogravimetric curves (Figure 7) that compounds **3** and **4** lose the water of crystallization completely by about $300\text{--}350^\circ C$. The observed values of percentage weight loss (6.8% for potassium and 6.4% for

(23) JCPDS Powder Diffraction File, Card No. 31-874.

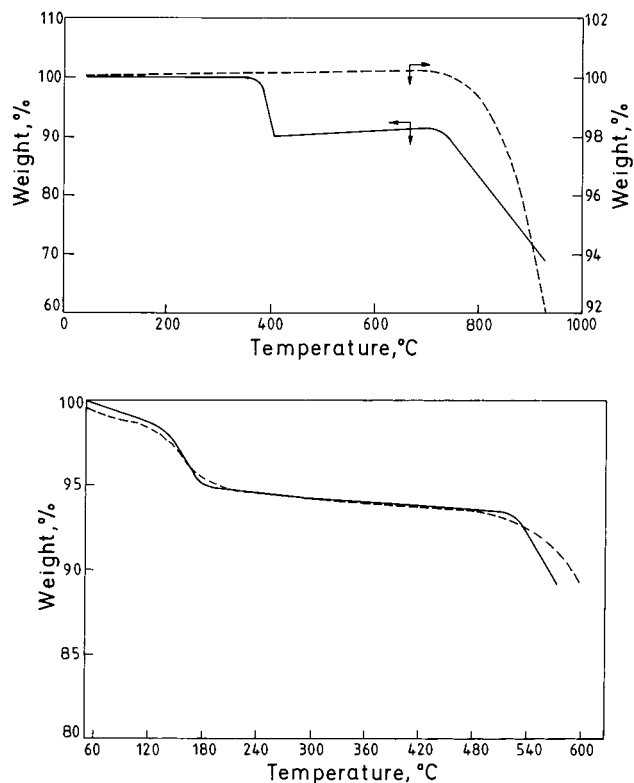


Figure 7. Thermogravimetric curves for the compounds $(NH_4)_2Mo_3TeO_{12}$ (—) and $Cs_2Mo_3TeO_{12}$ (---) (top) and the compounds $Rb_4Mo_6Te_2O_{24} \cdot 6H_2O$ (—) and $K_4Mo_6Te_2O_{24} \cdot 6H_2O$ (---) (bottom).

rubidium) correspond to loss of 5.5–6 molecules of water per formula unit and thus corroborate the crystallographic formulas. They undergo further weight loss at about $500^\circ C$ due to loss of volatile component oxides. DSC studies on these two compounds in a nitrogen atmosphere showed two endo and one exothermic peaks at temperatures of about 250 , 460 , and $320^\circ C$, respectively. The bulk samples were heated separately in a furnace in nitrogen and in open air. When the samples were heated at $470^\circ C$ in flowing N_2 , greenish yellow melts were obtained. The products of decomposition in open air at $450^\circ C$ were found to contain mainly $A_2Mo_3O_{10}$ ($A = Rb, K$)²⁴ phases.

Spectroscopic Studies. The infrared and Raman spectra of layered tellurite **1** and "zero-dimensional" tellurite **3** are given in Figure 8. Here we assign only selected frequencies based on the limited literature available on the spectral characteristics of tellurites. The infrared spectra of compounds **1** and **2** are similar to those of the corresponding selenites.⁶ The peaks at 3153 and 2779 cm^{-1} in the infrared spectrum of compound **1** can be ascribed to the symmetric ν_1 and asymmetric ν_3 stretches of the tetrahedral ammonium ion,²⁵ and the sharp peak at 1411 cm^{-1} is due to its asymmetric ν_4 stretch. The peaks at 907 and 857 cm^{-1} can be assigned to $Mo\text{--}O$ vibrations.²⁶ The peaks at 715 and 657 cm^{-1} could be due to one or more of the vibrations of $Mo\text{--}O$, $Te\text{--}O$, and $Mo\text{--}O\text{--}Te$, all of which fall in this range.^{26–28} The infrared spectrum of compound **2** is similar to that of **1**, and the peaks in the $1000\text{--}500\text{ cm}^{-1}$ range

(24) (a) JCPDS Powder Diffraction File, Card No. 36-337. (b) JCPDS Powder Diffraction File, Card No. 37-1467.

(25) Nakamoto, K. *Infrared Spectra of Inorganic and Coordination Compounds*; Wiley-Interscience: New York, 1970.

(26) Bart, J. C. J.; Cariati, F.; Sgamellotti, A. *Inorg. Chim. Acta* **1979**, *36*, 105.

(27) Dimitriev, Y.; Bart, J. C. J.; Dimitrov, V.; Arnaudov, M. Z. *Anorg. Allg. Chem.* **1981**, *479*, 229.

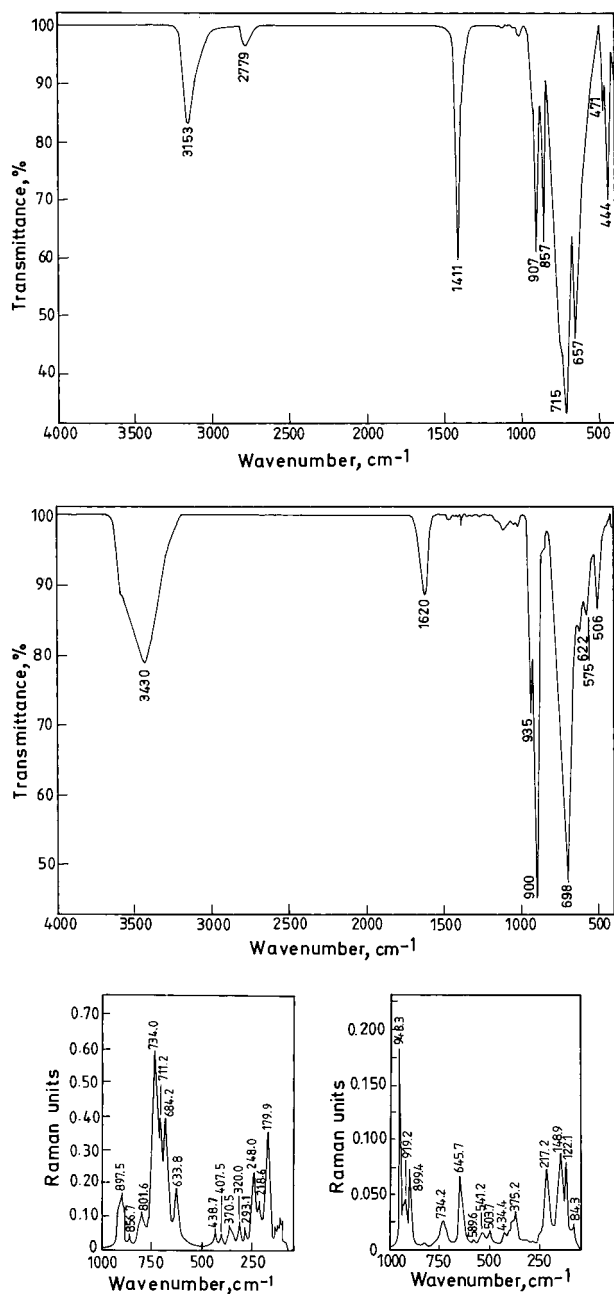


Figure 8. Infrared and Raman spectra of $(\text{NH}_4)_2\text{Mo}_3\text{TeO}_{12}$ (top; bottom left) and $\text{Rb}_4\text{Mo}_6\text{Te}_2\text{O}_{24}\cdot 6\text{H}_2\text{O}$ (middle; bottom right).

can be assigned similarly. The broad band around 3430 cm^{-1} in the infrared spectrum of compound **3** can be assigned to the antisymmetric and symmetric O–H stretchings and the peak around 1620 cm^{-1} to the HOH bending modes of lattice water. The peaks at 935 and 900 cm^{-1} can be assigned to Mo–O

vibrations whereas the peak at 698 cm^{-1} could be due to one or both of Mo–O and Te–O vibrations since this is an overlapping region for these vibrations. The infrared spectrum of **4** is similar to that of compound **3**.

The Raman spectrum of compound **1** is similar to that of **2**. Similarly, there is a close resemblance between the Raman spectra of **3** and **4**. The bands around 897 and 857 cm^{-1} in the Raman spectrum of compound **1** and the peaks around 948 , 919 , and 899 cm^{-1} in the Raman spectrum of compound **3** can be assigned to Mo–O vibrations whereas the bands in the 734 – 630 cm^{-1} range could be due to either Mo–O or Te–O vibrations or both.

Concluding Remarks

New noncentrosymmetric layered tellurites, $(\text{NH}_4)_2\text{Mo}_3\text{TeO}_{12}$ and $\text{Cs}_2\text{Mo}_3\text{TeO}_{12}$, isostructural with the corresponding selenites, have been prepared by hydrothermal methods. The two-dimensional $(\text{Mo}_3\text{TeO}_{12})^{2-}$ anion has an MoO_4 layer whose motif is based on a slice of hexagonal tungsten oxide structure. This layer is capped asymmetrically by tellurium on only one side. The cations NH_4^+ and Cs^+ have been found to be immobile. Similar layered tellurites of rubidium and potassium could not be synthesized.

Simple refluxing procedures yield the entirely new “zero-dimensional” compounds $\text{Rb}_4\text{Mo}_6\text{Te}_2\text{O}_{24}\cdot 6\text{H}_2\text{O}$ and $\text{K}_4\text{Mo}_6\text{Te}_2\text{O}_{24}\cdot 6\text{H}_2\text{O}$ containing discrete centrosymmetric $(\text{Mo}_6\text{Te}_2\text{O}_{24})^{4-}$ anionic aggregates and alkali metal ions. The anion contains a flat hexagonal Mo_6O_{24} ring formed by edge sharing of six MoO_6 octahedra, and these rings are capped on both sides by tellurium. The two types of anions of these four compounds have the same empirical formula, $(\text{Mo}_3\text{TeO}_{12})^{2-}$.

$\text{Cs}_2\text{Mo}_3\text{TeO}_{12}$, unlike the other three tellurites (**1**, **3**, and **4**), is stable at temperatures as high as $500\text{ }^\circ\text{C}$ and therefore could be prepared even by a solid-state reaction. This observation has led us to attempt the solid-state synthesis of bicapped tellurites and selenites of niobium, tantalum, vanadium and antimony. This alternative synthetic route has in fact paved the way for a simple and elegant synthesis of a host of other tellurites. We have completed the synthetic and structural investigation of the corresponding tungsten(VI) tellurites also for the purpose of comparative study. Our synthetic and structural investigations of all these new phases will be reported elsewhere.

Acknowledgment. We thank the Regional Sophisticated Instrumentation Center at our institute and the National Diffractometer Facility at the University of Mysore for single-crystal X-ray data collection. We also thank the Department of Science and Technology, India, for financial support.

Supporting Information Available: Tables of least-squares planes for **3** and **4** (4 pages). X-ray crystallographic files, in CIF format, for **1**–**4** are available on the Internet only. Ordering and access information is given on any current masthead page.

(28) Arnaudov, M.; Dimitrov, V.; Dimitriev, Y.; Markova, L. *Mater. Res. Bull.* **1982**, *17*, 1121.